Structure and electronic properties of ultrathin gold films on vicinal silicon(111)

ARTICLE *in* THIN SOLID FILMS · MARCH 2003

Impact Factor: 1.76 · DOI: 10.1016/S0040-6090(02)01248-8

Available online at www.sciencedirect.com
SCIENCE DIRECT®
Thin Solid Films 428 (2003) 11–14
thin solid films
www.elsevier.com/locate/tsf

Structure and electronic properties of ultrathin gold films on vicinal silicon(111)

M. Schöck[a], C. Sürgers[a,*], H. v. Löhneysen[a,b]

[a]*Physikalisches Institut and Center for Functional Nanostructures, Universitat Karlsruhe, D-76128 Karlsruhe, Germany*
[b]*Forschungszentrum Karlsruhe, Institut fur Festkorperphysik, D-76021 Karlsruhe, Germany*

Abstract

The surface of vicinal Si(111) with a misorientation of 10° towards the azimuthal $[\overline{1}12]$ direction is investigated by scanning tunneling microscopy and spectroscopy before and after submonolayer deposition of Au. For 0.2 and 0.4 ML coverage, the surface structure shows domains corresponding to Si(557) facets with chain-like protrusions and rows extending along the step edges. Tunneling spectra taken above the protrusions clearly reveal different electronic properties of Si(557):Au in contrast to the bare Si(111)-(7×7) surface. In particular, for tunneling voltages $|U|>0.5$ V the spectra do not show any distinct features which suggests the presence of electronic bands with a smooth dispersion. The temperature dependence of the surface conductance indicates a non-metallic behavior for the bare Si(111)-(7×7) surface and for Si(557):Au-0.2 ML. For 0.4 ML an anisotropic conductance is measured which depends on the direction of the current with regard to the step edges.

PACS: 68.37.Ef; 73.25.-hi; 73.63.-b; 81.16.Dn

Keywords: Scanning tunneling microscopy; Scanning tunneling spectroscopy; Silicon surfaces; Si(111):Au reconstruction

1. Introduction

Vicinal surfaces can be used as templates for the synthesis of metallic nanostructures at the atomic level. For instance, gold on vicinal Si(111) exhibits different Au-induced reconstructions depending on miscut angle and Au coverage. A previous scanning tunneling microscopy (STM) study has shown that for a submonolayer coverage the Au-adsorbed terraces can be classified into three types depending on the terrace widths and on the structures on adjacent terraces [1]. Broad terraces exhibit the Si(111)-(5×2):Au reconstruction with one-dimensional row structures along the step edges, i.e. along the [110] direction, which are also observed on flat substrates for 0.2–0.5 monolayers (ML) Au [2,3]. Due to the missing correlation between the rows this phase is identified as a (5×1) reconstruction in low-energy electron diffraction [2]. Remarkably large domains of the 5×2 phase can be stabilized by the intentional miscut in $[\overline{1}12]$ direction, which then serves as a playground for the study of the electronic properties of a quasi-one-dimensional system [4–6].

On narrow terraces, which also appear on oriented Si(111) substrates with a large miscut angle, the surface structure corresponds to the Si(557):Au facet with single rows parallel to each step, which show a high degree of ordering for 0.2 ML Au [7]. Beyond 0.2 ML up to 0.5 ML the $\left(\sqrt{3}\times\sqrt{3}\right)$R30° reconstruction evolves. The lower optimum coverage of 0.2 ML for the Si(557):Au facet is consistent with the fact that the unit cell contains only one row of Au atoms plus an atomic step compared to the Si(111)-(5×2):Au reconstruction, where the unit cell contains two rows of Au separated by a single Si row-spacing. Structural investigations and first-principle calculations suggest that the step edge is an unfavorable location for Au atoms which is in contrast to the simple picture of step decoration [8,9].

Both Au-induced nanostructures have recently attracted considerable interest due to their different unusual electronic properties which are ascribed to the quasi-one-dimensional character of the surface structure [5]. Concerning the (557) facet, the interpretation of photo-

*Corresponding author. Tel.: +49-721-608-3456; fax: +49-721-608-6103.
E-mail address: christoph.suergers@physik.uni-karlsruhe.de (C. Sürgers).

0040-6090/03/$ - see front matter © 2002 Elsevier Science B.V. All rights reserved.
PII: S0040-6090(02)01248-8

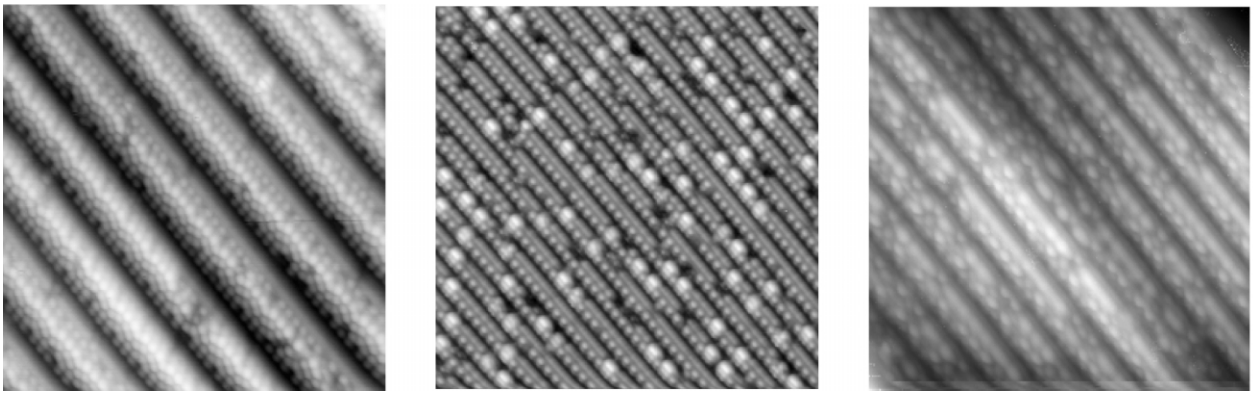

Fig. 1. STM images of vicinal Si(111) misoriented by 10° towards [112]. Left: Bare Si(111) surface with 7×7 reconstruction after heating up to 1000 °C (30 nm×30 nm). Center: Si(557):Au after deposition of 0.2 ML Au (30 nm×30 nm). Right: Si(557):Au after deposition of 0.4 ML Au (20 nm×20 nm).

emission data is controversial, indicating either spin-charge separation in a Luttinger liquid [10] or two half-filled nearly degenerate surface-state bands which give rise to a metallic surface [11]. The latter proposal is compatible with first-principle calculations [9].

Up to now, most of the work concentrated on the surface and electronic structure investigated by STM or photoemission. Although STM imaging at different tunneling voltages has been performed earlier, scanning tunneling spectroscopy (STS), i.e. $I-U$ measurements, have not been carried out so far. Here we report on STS data of the Au-induced (557) facet obtained on highly miscut Si(111) substrates which show distinct differences in comparison to the bare Si surface, and present first electrical transport measurements.

2. Experimental

n-type Si(111) substrates (P doped, resistivity 5 Ωcm) with an intentional miscut of 10° from the [111] axis towards the $[\bar{1}\bar{1}2]$ azimuthal direction were heated to 750 °C several times and finally flashed to 1000 °C by electron-beam heating in ultra-high vacuum for cleaning and desorption of the native oxide layer. Au was deposited by either thermal or electron-beam evaporation. The Au coverage was determined from the evaporation time and rate (typically <0.1 ML/min) which was determined with a calibrated quartz oscillator. Electrochemically etched tungsten tips were cleaned in situ by several cycles of Ar^+ ion bombardment and annealing. All STM images presented here were taken at room temperature in constant current mode at a voltage of $+0.9$ V applied to the sample. In addition, current–voltage ($I-U$) curves were taken at selected points of the surface. The derivative dI/dU was measured simultaneously with a lock-in amplifier operating at a frequency of 3.43 kHz with a modulation amplitude of 20–40 mV. During ramping the voltage, the tip was retracted from the surface with a constant rate to avoid field-emission between the tip and the sample at high bias. Tunneling spectra $(dI/dU)/(I/U)$ were calculated from the data to minimize the influence of the varying tip-sample separation.

Resistance measurements were performed in-situ for temperatures $T=1.8-300$ K with an ac-resistance bridge. For this purpose, 10-nm-thick gold pads were evaporated separately through a 3-μm-thick glass wire serving as a shadow mask in front of the sample. For the four-point probe measurements spring-loaded needles were pressed onto the gold pads for electrical contact.

3. Results and discussion

After flash heating and prior to Au deposition, the STM image (Fig. 1, left) shows equidistant steps of nearly equal height running along [110]. The terraces exhibit the Si(111)-(7×7) reconstruction which is generally observed after heating to temperatures beyond 500 °C. The image taken at $+0.9$ V is compatible with earlier STM investigations, where the recorded images are in accordance with the dimer-adatom-stacking fault model of the 7×7 surface [12].

Evaporation of gold at a substrate temperature $T_s=$ 550 °C, corresponding to a coverage of 0.2 ML, and subsequent annealing to $T_s\approx750$ °C results in the formation of large domains exhibiting a one-dimensional surface structure with rows extending along the [110] direction, i.e. parallel to the step edges (Fig. 1, center). The characteristic substructure consists of single bright protrusions arranged in chains adjacent to blurred rows. We mention that the chain-like protrusions are generally observed on all samples at 0.2 ML coverage, whereas the appearance of the rows seems to depend on the quality, i.e. sharpness and/or cleanness, of the tunneling tip. Similar STM images of the Si(557):Au have been reported earlier [1,11] without an unequivocal attribution

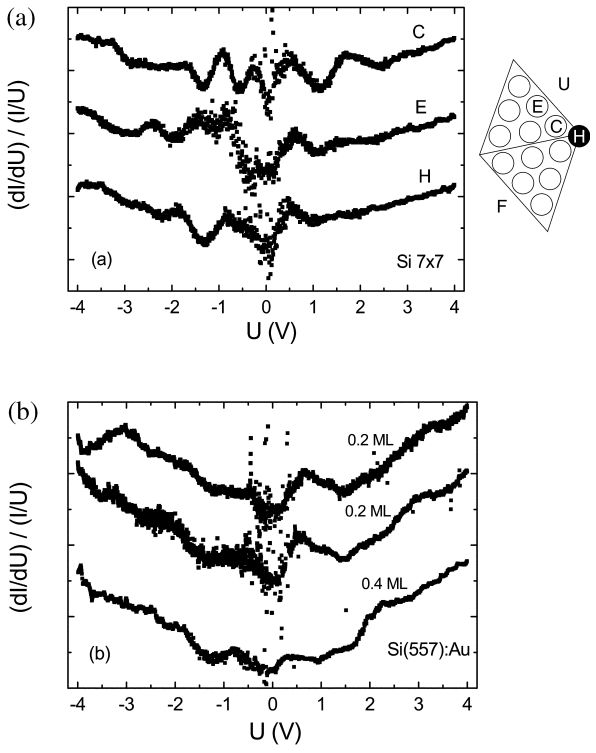

Fig. 2. Tunneling spectra $(dI/dU)/(I/U)$ vs. tunneling voltage U taken on (a) 10°-miscut Si(111) and (b) Si(557):Au with 0.2 ML and 0.4 ML Au. Letters indicate spectra taken at different points on the unfaulted (U) or faulted (F) half of the Si(111)-(7×7) unit cell; see sketch.

of the observed structures to Si or Au. For a higher coverage of 0.4 ML the one-dimensional surface structure remains stable on regions with a high density of steps (Fig. 1, right), i.e. on narrow terraces. However, for this coverage (larger than the optimum of 0.2 ML for the Si(557):Au structure) we also observe domains of the $\left(\sqrt{3}\times\sqrt{3}\right)$R30° reconstruction on broader terraces (not shown) [7,10].

Fig. 2 shows representative tunneling spectra $(dI/dU)/(I/U)$ taken on the different surfaces. On the bare vicinal Si(111) (Fig. 2a), the spectra show well resolved features characteristic for the 7×7 reconstruction [12]. Different spectra are found at selected tip positions (corner adatom C, edge adatom E, and corner hole H) of the 7×7 unit cell. These can be ascribed to distinct occupied and unoccupied electronic states also observed in photoemission.

Spectra taken on the chain-like protrusions of the Si(557):Au surface are remarkably different (Fig. 2b), For 0.2 ML Au, two peaks separated by $\Delta E \approx 1$ V are observed near the Fermi level, i.e. at $U \approx \pm 0.5$ V. Apart from these two peaks, the spectra are featureless suggesting the lack of narrow electronic bands with a high local density of states contributing to the tunneling current. It is reassuring that spectra taken on specific points on Si(557):Au domains are independent of the coverage (cf. 0.2 ML and 0.4 ML) regardless of the above-mentioned presence of $\left(\sqrt{3}\times\sqrt{3}\right)$R30° domains for 0.4 ML Au. This demonstrates the advantage of STS as a local probe for electronic properties.

When comparing these results with photoemission data one has to keep in mind that for small voltages, i.e. at energies near the Fermi level, the tunneling current is dominated by contributions from electronic states near the Γ-point, i.e. with a wave vector $k_{||}=0$ or by states of a high local density of states, for instance electronic surface states or nearly localized states originating from a d band. However, at higher voltages states with $k_{||}\neq 0$ may also contribute to the tunneling current. Most of the recent photoemission experiments concentrate on regions near the Brillouin zone edge [5,10,11]. However, it is motivating that a recent first-principle calculation obtains bands with a strong dispersion which are derived from 3sp bonds of Si atoms [9], Recent X-ray diffraction data also suggest the assignment of the prominent features seen in STM to Si atoms [8]. Clearly, further atomically resolved STS measurements are necessary for a verification of the electronic structure of Si(557):Au together with an individual discrimination of the two types of substructures, i.e. chains and rows, and their electronic properties.

Fig. 3 shows the temperature dependence of the surface conductance $G_{\square}=t/wR$ (t, contact distance; w, contact width; R, resistance) normalized to the value at $T=290$ K vs. $1/T$ for temperatures T above 30 K. For lower temperatures the sample resistance increased beyond 2 MΩ, and could not be measured anymore by the experimental set-up. All samples show a decreasing

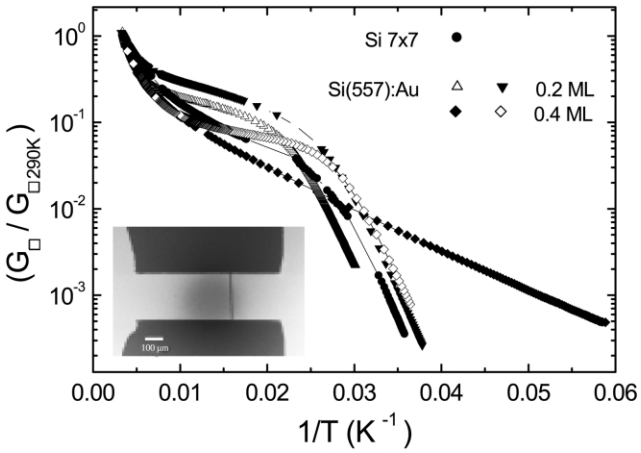

Fig. 3. Normalized surface conductance $G_{\square}(T)/G_{\square}$ (290 K) vs. inverse temperature $1/T$ for the different samples. For 0.4 ML Au, (♦) represents data with the current applied parallel to the step edge, whereas (◇) represents data with the current applied perpendicular to the step edges. The inset shows an electron micrograph of the gold pads deposited prior to the resistance measurement.

conductance with decreasing temperature, i.e. a non-metallic behavior.

For 0.2 ML, the overall temperature dependence is similar to the bare Si substrate. The observation of non-metallic $R(T)$ behavior has different reasons. First, the one-dimensional structures could be electrically broken by large defects such as steps or dislocations. This requires further measurements with a smaller electrode-to-electrode distance down to the sub-micrometer range. Secondly, assuming a metallic surface, the presence of delocalized states at the Fermi level does not inherently give rise to a high electrical conductivity. In case of electronic bands with a high effective mass this results in a small contribution to the conductivity. Similar arguments have been put forward to explain the low conductivity of the 'metallic' Si(111)-(7×7) surface [13].

For 0.4 ML, the temperature behavior is very different compared to 0.2 ML if the current is applied parallel to the step edges (♦) whereas a similar behavior as for 0.2 ML is obtained if the current is applied perpendicular to the step edges (◇). This demonstrates a high anisotropy of the electrical conductivity presumably due to the one-dimensional structure. However, for 0.4 ML the surface also exhibits domains of the $\left(\sqrt{3}\times\sqrt{3}\right)$R30° on broader terraces as mentioned above, which also can contribute to the conductance in an unknown way. For a full description of the surface conductance the effects of the coverage on the surface state bands and on the surface space-charge layer have to be taken into account. The latter has been considered earlier to be the most prominent for explaining the surface conductivity of the Si(111)-(5×2) reconstruction at room temperature [13].

4. Conclusions

Scanning tunneling spectra taken on Si(557):Au exhibit features which seem to be characteristic for the one-dimensional structures usually observed in the STM images. These features are attributed to electronic states calculated in recent band-structure calculations. A possible assignment of these spectra to the distinct structures in the domains must await further STS measurements. Preliminary conductance measurements well below room temperature indicate a non-metallic behavior which, however, could be due to the presence of macroscopic defects. For a detailed analysis of the electrical transport further measurements will be done.

Acknowledgments

This work was supported by the DFG through SFB 195 and the Center for Functional Nanostructures. We thank P. Pfundstein for performing the electron microscopy measurements.

References

[1] M. Shibata, I. Sumita, M. Nakajima, Phys. Rev. 57 (1998) 1626.
[2] A.A. Baski, J. Nogami, C.F. Quate, Phys. Rev. B 41 (1990) 10247.
[3] L. Seehofer, S. Hubs, G. Falkenberg, R.L. Johnson, Surf. Sci. 329 (1995) 157.
[4] I.R. Collins, J.T. Moran, P.T. Andrews, R. Gosso, J.D. O'Mahony, J.F. McGilp, G. Margaritondo, Surf. Sci. 325 (1995) 45.
[5] K.N. Altmann, J.N. Crain, A. Kirakosian, J.-L. Lin, D.Y. Petrovykh, F.J. Himpsel, R. Losio, Phys. Rev. B 64 (2001) 035406.
[6] J.D. O'Mahony, J.F. McGilp, C.F.J. Flipse, P. Weightman, F.M. Leibsle, Phys. Rev. B 49 (1994) 2527.
[7] M. Jałochowski, M. Strożak, R. Zdyb, Surf. Science 375 (1997) 203.
[8] I.K. Robinson, P.A. Bennett, F.J. Himpsel, Phys. Rev. Lett. 88 (2002) 096104.
[9] D. Sánchez-Portal, J.D. Gale, A. Garcia, R.M. Martin, Phys. Rev. B 65 (2002) 081401.
[10] P. Segovia, D. Purdie, M. Hengsberger, Y. Baer, Nature 402 (1999) 504.
[11] R. Losio, K.N. Altmann, A. Kirakosian, J.-L. Lin, D.Y. Petrovykh, F.J. Himpsel, Phys. Lett. 86 (2001) 4632.
[12] R.J. Hamers, R.M. Tromp, J.E. Demuth, Phys. Rev. Lett. 56 (1986) 1972.
[13] C.-S. Jiang, S. Hasegawa, S. Ino, Phys. Rev. B 54 (1996) 10389.